N90-28297

IR Spectral Characteristics of Cirrus Clouds

Steven A. Ackerman and William L. Smith

Cooperative Institute for Meteorological Satellite Studies

Space Science and Engineering Center, 1225 West Dayton St.

University of Wisconsin-Madison, Madison, WI. 53706

(July 1989)

The recent focus of parameterizations of the radiative properties of clouds has been to include the microphysical properties of the cloud. A variety of parameterizations have been developed for both the shortwave and the longwave. In parameterizing the longwave properties of clouds, it is useful to consider the two stream solution of the radiative transfer equation appropriate for a thermal source. While various solutions exist, here we consider the form

$$\begin{bmatrix} F^+(\tau_b) \\ F^-(\tau_t) \end{bmatrix} = \begin{bmatrix} t & r \\ r & t \end{bmatrix} \begin{bmatrix} F^+(\tau_t) \\ F^-(\tau_b) \end{bmatrix} + \begin{bmatrix} s-t & 1-s-r \\ 1-s-r & s-t \end{bmatrix} \begin{bmatrix} B(\tau_t) \\ B(\tau_b) \end{bmatrix} \tag{1}$$

where

$$r = \frac{\rho(1-e^{-\tau_{eff}})}{1-\rho^2 e^{-\tau_{eff}}} \tag{2}$$

$$t = \frac{e^{-\tau_{eff}}(1-\rho^2)}{1-\rho^2 e^{-\tau_{eff}}} \tag{3}$$

$$s = \frac{(1-t+r)}{\bar{\mu}(1-\omega_0+2\omega_0\bar{\beta})r} \tag{4}$$

$$K = \sqrt{1 - 2\omega_0 + \omega_0^2 + 2\omega_0\bar{\beta} - 2\omega_0^2\bar{\beta}} \tag{5}$$

$$\tau_{eff} = \bar{\mu}K\tau = \pi\bar{\mu}\int\int KQ_{ext}\mathrm{n(r)r^2\,dr\,dz} \tag{6}$$

$$\rho = \frac{\omega_0\bar{\beta}}{1-\omega_0+\omega_0\bar{\beta}+K} \tag{7}$$

PRECEDING PAGE BLANK NOT FILMED

where B is the Plank function $\bar{\beta}$ is the backscatter coefficient and $\bar{\mu}$ is the diffusivity factor ($\bar{\mu} \approx 1.66$). For an isothermal cloud, $B(\bar{\tau})$, equations (12)-(18) indicate the necessity to parameterize two variables, ρ and KQ_{ext}. Physically, ρ is the reflectance for an infinitely thick cloud. The value of ρ as a function of wavelength is shown in figure 1 for ice spheres. For wavelengths between 10 and 13μm, ρ is a weak function of the particle size and $\rho < 0.08$. ρ can become large for small particles for regions outside this window.

To parameterize KQ_{ext} we consider the ratio of KQ_{ext} to Q_{abs}. This ratio (Figure 2) displays a similar dependency on wavelength and particle size as that depicted by ρ, with a strong dependency on particle size outside the window region. For wavelengths between 10 and 13 μm, $KQ_{ext} \approx Q_{abs}$. In parameterizing the longwave properties of clouds in the 10-13 μm window region, it is therefore useful to parameterize Q_{abs}. An appropriate parameterization of Q_{abs} is that of the modified anomalous diffraction theory. Figure 3 depicts the relations between wavelength and Q_{abs} for two different droplet sizes. The stars represent Mie calculations while the circles denote the approximation of equation (9). The open symbols are for a 30μm particle while the solid symbols represent the calculations for a 1μm droplet. The approximation is excellent, even for droplets as small as 1μm.

The dependence of effective emittance on the particle size can be expressed to second order using MADT as

$$\varepsilon = 1 - \exp\left(\bar{\mu}\pi \int\int \mathrm{n(r)} \left\{\frac{4}{3}m^2 r^3 \kappa \left[1 - (1 - m^{-2})^{3/2}\right] \mathrm{dr} + \mathrm{r}^4\kappa^2 m^2 \left[1 - (1 - m^{-2})^2\right]\right\} \mathrm{drdz}\right)$$

where $\kappa = 4\pi n_i/\lambda$ is the absorption coefficient of water/ice. The first term of the exponential represents the dependency on the water content of the cloud, while the second term displays a dependency on the fourth moment of the size distribution. As an estimate of the particle size at which the emissivity becomes dependent on the droplet size we consider the radius at which

$$\frac{4}{3}m^2\kappa \left[1 - (1 - m^{-2})^{3/2}\right] = \mathrm{R}\kappa^2 m^2 \left[1 - (1 - m^{-2})^2\right] \tag{9}$$

Figure 4 depicts this radius, R, as a function of wavelength for water (solid lines) and ice (dashed lines) spheres. A cloud with a monomodal distribution of particles of size R or greater will display a sensitivity to droplet size. For example, if we have two water clouds, one with a monomodal size distribution of 12μm particle and the other with a 8μm droplet distribution, the cloud emissivity in the 8-11.5 μm band will be sensitive primarily to the LWP, while the 11.5 to 14 μm band emissivity would also display a sensitivity to the size distribution. This is in agreement measurements and calculations of fogs. In the the case of ice clouds, the 11- 13 μm band will display a dependency on the size distribution for particles greater than 4μm.

In summary, high spectral resolution measurements in the 8-13 μm "window" region are appropriate for remotely sensing the microphysical properties of ice clouds as: windows in gaseous absorption are available; this is the most sensitive region to particle size; the value of ρ is small compared to other wavelengths; and $KQ_{ext} \approx Q_{abs}$.

To demonstrate this dependency of particle size on IR observations, we consider the spectral variation of the equivalent blackbody temperatures in the "window" region, four spectral bandwidths: 8 μm (8.3-8.4), 10 μm (10.07-10.173), 11 μm (11.062-11.249) and 12 μm (11.93-12.063). The equivalent blackbody temperature observations were made with the HIS (High resolution Interferometer Spectrometer) aboard the NASA ER2 during FIRE on 2 November, 1986. Figure 5 is a scatter diagram of the BT_8-BT_{11} versus BT_{11}-BT_{12}. Each symbol in figure the figure represents a range in the BT_{11} as noted in the legend. The differences in the brightness temperatures observed in these channels are very useful in detecting the presence of cirrus clouds. The cloud free regions have negative differences in BT_8-BT_{11} due to absorption by water vapor. While cirrus clouds have positive differences owning to the optical properties of ice. The cirrus BT_8-BT_{11} are greater than the BT_{11}-BT_{12} as expected from figure 3.

The magnitude of the HIS measured BT differences is related to the cloud particle size distribution. This is demonstrated in figure 6 where the brightness differences are determined with theoretical radiative transfer calculations using a doubling/adding model and assuming various surface temperatures, cloud top temperatures, and different ice water content and geometric thicknesses. The cloud is assumed to have a lapse rate of -6 °K km^{-1} and is homogeneous. The cloud particles are assumed to be spheres with a gamma size distribution and effective radii as denoted in the symbol legend. These calculations demonstrate that the ice cloud with the smaller r_{eff} (stars) display the large BT differences observed by the HIS while the ice cloud with the larger r_{eff} do not. The magnitude of the ΔBT is also related to the IWP (e.g. very thin clouds are similar to the clear sky values.

The envelope of the calculations is depicted on figure 5 by the solid line. Differences between the theory and observations are seen at the larger BT_8-BT_{11} values. This difference may be attributed to particle shape, or to a non-homogeneous vertical/horizontal distribution of the particles. The effect of particle shape is demonstrated by the dashed line which is the envelop for a cirrus cloud consisting of small ice cylinders.

4. SUMMARY

- The HIS spectra show spectral variations in equivalent blackbody temperatures in the window region of greater than 5°C, for a given cirrus cloud.
- The brightness temperature differences between 8 and 11 μm and 11 and 12 μm are useful parameters for detecting the presence of cirrus clouds.
- Theoretical calculations indicate that the magnitude of the spectral variation in brightness temperature is related to the particle size. The smaller particles are associated with larger brightness temperature differences.
- The magnitude of the brightness temperature differences are also related to the particle shape. Calculations assuming spherical particles are in better agreement with the majority of HIS observations than similar calculations assuming cylindrical particles.

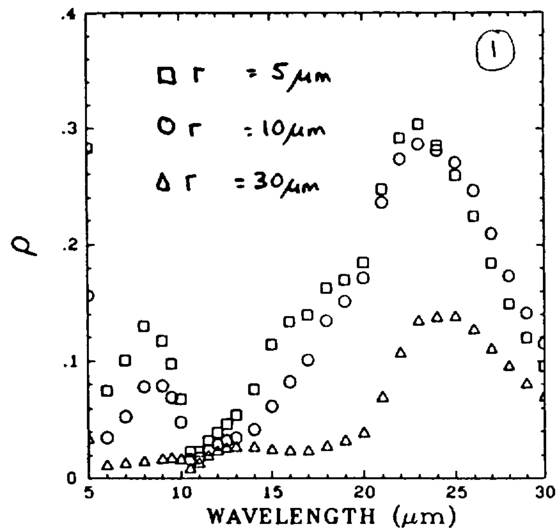

1
□ r = 5μm
○ r = 10μm
Δ r = 30μm
ρ
WAVELENGTH (μm)

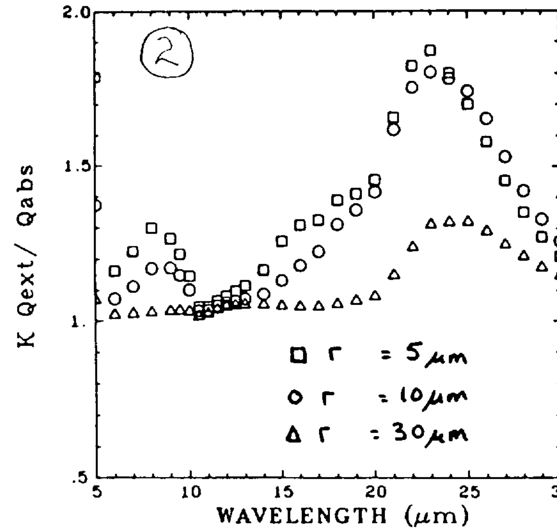

2
K Qext/ Qabs
□ r = 5μm
○ r = 10μm
Δ r = 30μm
WAVELENGTH (μm)

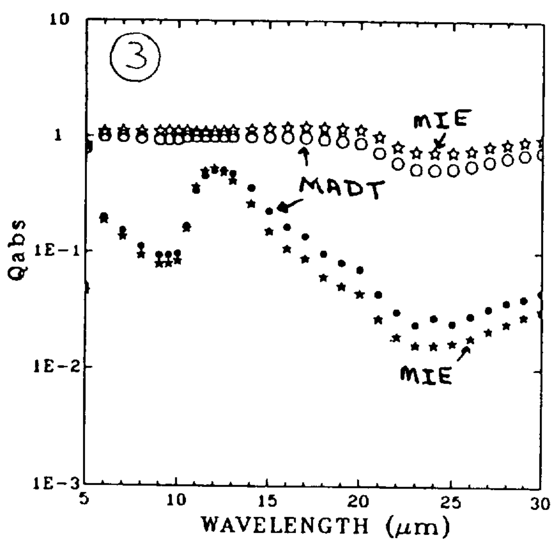

3
Qabs
MIE
MADT
MIE
WAVELENGTH (μm)

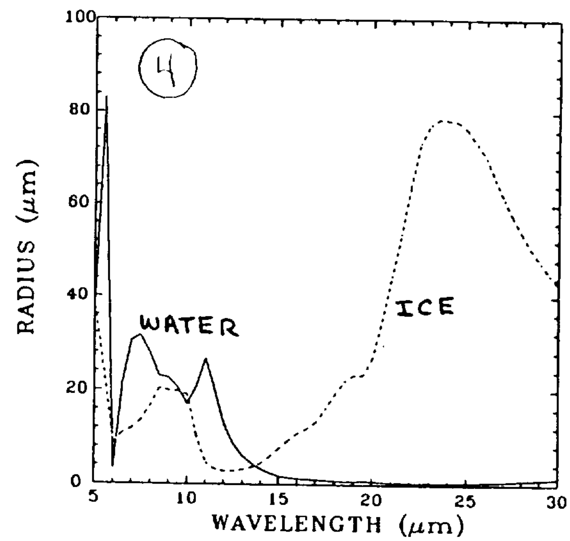

4
RADIUS (μm)
WATER
ICE
WAVELENGTH (μm)

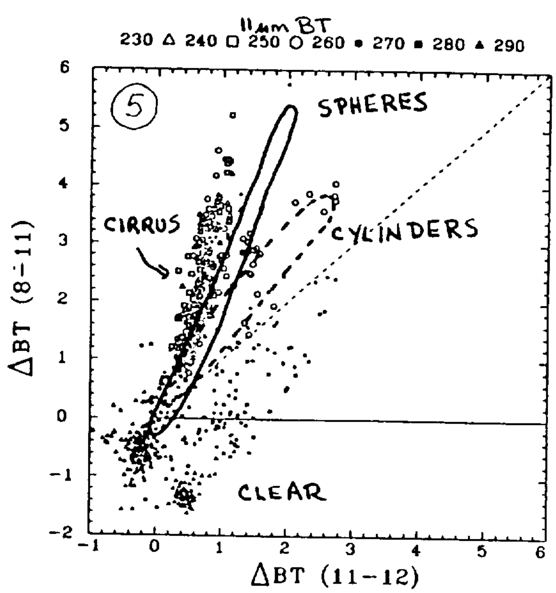

11μm BT
230 Δ 240 □ 250 ○ 260 • 270 ▪ 280 ▴ 290
5
SPHERES
CIRRUS
CYLINDERS
CLEAR
ΔBT (8-11)
ΔBT (11-12)

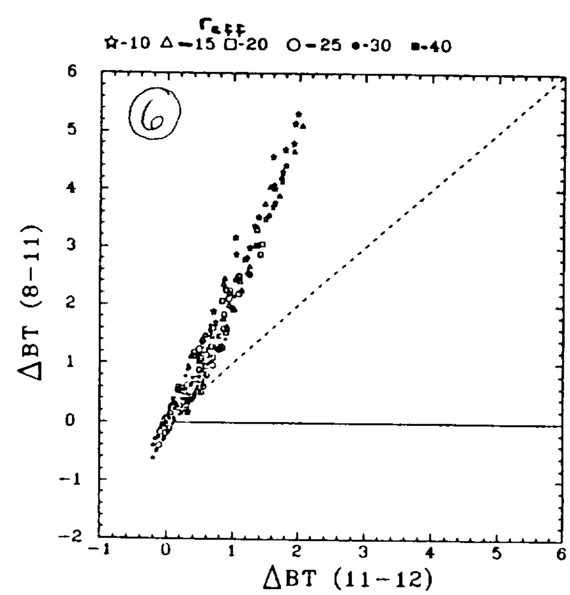

reff
☆-10 Δ-15 □-20 ○-25 •-30 ▪-40
6
ΔBT (8-11)
ΔBT (11-12)